Research Article

Imaging lateritic bauxite bearing zones in Ekiti, Southwestern Nigeria, using magnetic and electrical resistivity tomography techniques

Joel Olayide Amosun[1] · **Olufemi Adigun Alagbe**[2] · **Tokunbo Sanmi Fagbemigun**[1] · **Oluseun Adetola Sanuade**[3] · **Olayiwola Grace Olaseeni**[1]

Received: 29 April 2020 / Accepted: 29 October 2020 / Published online: 20 November 2020

Abstract

This research uses geophysical techniques such as magnetic and electrical resistivity tomography to image the lateritic bauxite bearing zones in Orin Ekiti, Southwestern Nigeria. The high-resolution aeromagnetic data were utilized for generating the total magnetic intensity (TMI) map. Different filtering techniques such as Euler deconvolution and total horizontal derivative were also carried out to enhance better understanding of bauxite deposit, with the generation of different maps therein. Low magnetic intensities were observed over charnockitic rock which is a host material for bauxite occurrence. Magnetic low trending NE–SW was observed in the study area. The (EUD and THDR) maps were then superimposed on the geologic map to geo-reference areas that have dominant charnockite. The depth extent and structural signature interpreted from magnetic interpretations show that significant deposit in the study area is at shallow depth which tallies with the geology of bauxite as being a supergene enrichment (surficial deposit). 2D ERT results obtained from five traverses with inter-traverse separation of 45 m and traverse length of 100 m each, established in the NW–SE direction to image the lateritic bauxite deposit based on the prospect shown from the aeromagnetic analysis. The images display the constant resistivity regimes beneath the traverses with different colour bands. The 2D ERT profiles and 3D inversion results show bauxitic zones to be of high resistivity which ranges from 154 to 3814 Ω m, the migmatite gneiss and granitic rocks (unaltered parent rocks) are of considerably lower resistivity than the weathered charnockitic rock and by extension bauxitic zones. These different techniques used in this study have however shown that the area of interest for bauxitic deposit in Orin Ekiti trends in the NE–SW direction with a dominant concentration in the northeastern (NE) part. By the same token, this research has been able to substantiate the fact that bauxite deposits occur as supergene enrichment.

Keywords Lateritic bauxite · Magnetic · Charnockite · Near-surface geophysics

1 Introduction

The solid mineral sector has been the driving force for economic growth in most country of the world including Nigeria. Minerals are the constituent of rocks, ores and meteorites, and with a few exceptions, they are the most stable chemical elements known to man [1]. Solid mineral development has been known to be associated with a lot of difficulties and challenges ranging from location accessibility, availability of surveying and analyzing equipment, to cost and stress of collecting, processing and interpreting data. Among several mineral deposits in Nigeria, bauxite deposits are found mainly in four states of the

✉ Joel Olayide Amosun, joelamosun@gmail.com | [1]Department of Geophysics, Federal University Oye Ekiti, Oye, Nigeria. [2]Department of Applied Geophysics, Federal University of Technology Akure, Akure, Nigeria. [3]Boone Pickens School of Geology, Oklahoma State University, Stillwater, OK, USA.

federation and they are Plateau, Ondo, Ekiti and Adamawa states [2].

Bauxite is a naturally occurring material that is made of diverse composition that is relatively rich in aluminium. It contains 40–60 per cent aluminium oxide (Al_2O_3), 9–18 per cent iron oxide (Fe_2O_3), 2–9 per cent titanium oxide (TiO_2) and 1.5–4.5 per cent silicon oxide (SiO_2). The major minerals found in bauxite are boehmite ($Al_2O_3{\cdot}H_2O$), gibbsite ($Al_2O_3{\cdot}3H_2O$) and diaspora, plus a minor quantity of iron oxides [goethite (FeO (OH)) and haematite (Fe_2O_3)] with trace amounts of silica (SiO_2) and anatase (TiO_2) [3]. Bauxite is an important raw material of aluminium, the metal used for soft drink cans to jumbo jets, non-metallurgical operations for the manufacture of refractories, abrasives, alumina chemicals and cement industry. It also found usefulness in cement and chemical industries, and in the production of dishwashers, it can also be used as a raw material in the commercial production of aluminium metal and alumina (Al_2O_3) [4]. Therefore, given the huge economic importance of bauxite as enumerated above and researches that have been conducted to establish the occurrence of lateritic bauxite deposit in Orin Ekiti by different authors [4–6], this study is aimed at imaging the subsurface settings of lateritic bauxite deposit in Orin Ekiti, Southwestern Nigeria, using aeromagnetic and electrical resistivity tomography (ERT) techniques and also delineate other potential zones in the area for further studies.

2 Site description and geology of the study area

Orin Ekiti is about 38.8 km from Ado Ekiti (Fig. 1) and lies on latitude 7°45′0.00′′–7°55′0.00 N and longitude 5°10′0.00″E–5°20′0.00″ E with terrain that is gently undulating. The topographic elevation of the area ranges between 535 and 644 m above sea level. Its climate is characterized by dry and wet season which the dry, which come up around November and March; and December and January, respectively. The peak rainfall is recorded in July and September. The average annual rainfall is 1333.2 mm, the annual temperature is 33 °C while the minimum is 18 °C. The main rock types in the study area are granite gneiss, banded gneiss, granite, migmatite and charnockite (Fig. 2). Largely, the study area is rugged with outcrops of charnockite in some locations [4].

3 Methodology

Two geophysical methods were employed for this study; the magnetic and the electrical resistivity methods. The magnetic method involved the use of high-resolution aeromagnetic data (HRAD), while the electrical resistivity method employed the use of electrical resistivity tomography (ERT) involving Wenner array.

Aeromagnetic data were acquired by a company known as Fugro Airborne Survey Limited as a direction by the Nigerian Geological Survey Agency (NGSA) between 2003 and 2009 which was aimed at promoting and assisting with mineral prospecting in Nigeria. The data acquisition

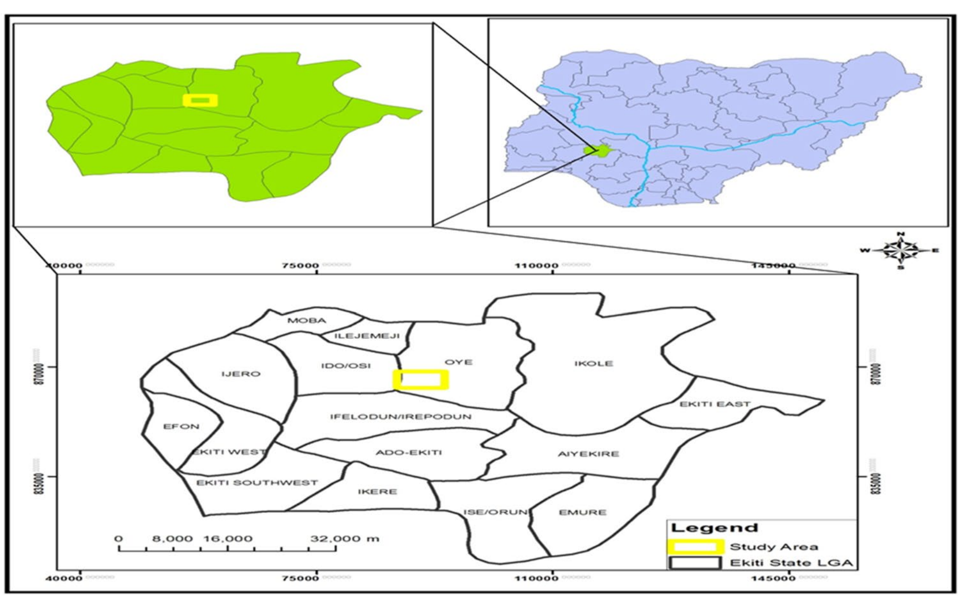

Fig. 1 Map showing the study area

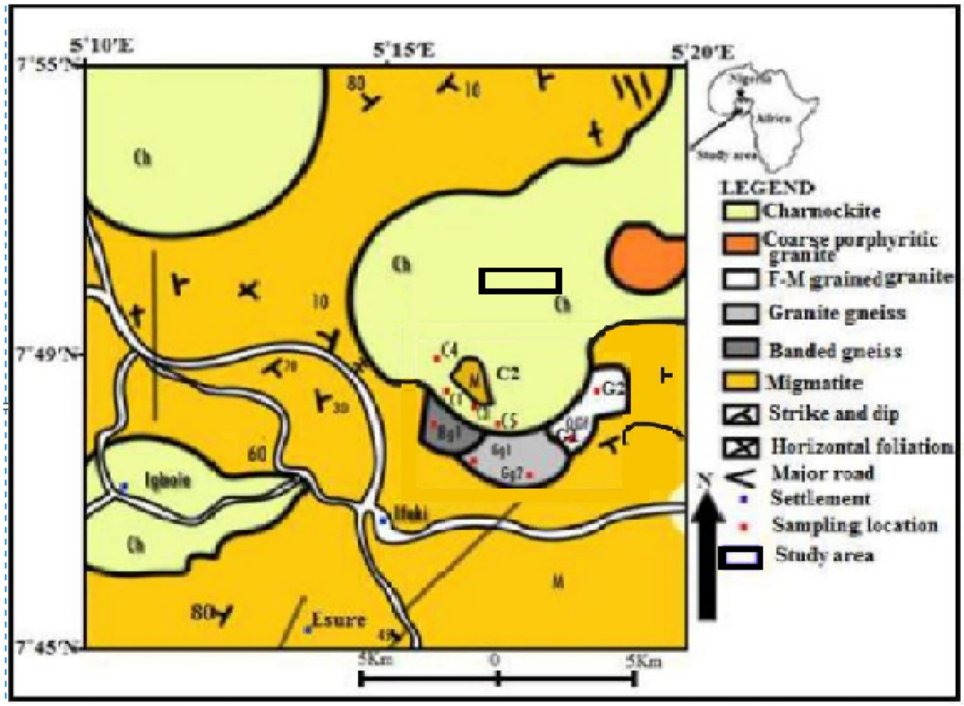

Fig. 2 Geologic map showing the rock types [4]

was carried out by aircraft covering 235,000 line kilometres with terrain clearance of 80 m and a flight spacing of 200 m. The direction of the flight was in NW–SE with a tie-line spacing of 200 m and tie-line direction of NE–SW. The data were corrected regionally based on the international geomagnetic reference field (IGRF) model 1984. Gridding of the data was also carried out using cell sizes of 1000 m.

The aeromagnetic data sheet 244 from NGSA is fed into the Oasis Montaj software where the TMI map will be generated from the given data. The data have to be reduced to the equator (Nigeria being in low magnetic latitudes) to centre the peaks of magnetic anomalies over their sources. This enhanced the data interpretation without losing any geophysical meaning, after which regional and residual separation is carried out. The residual map produced was then worked on to perform the necessary filtering techniques such as EUD [7], with structural index (SI) of 0.5 [8] to generate the depth to the anomaly.

The total horizontal derivative (THDR) [9] and lithologic contact between different rock types in the study area were established using EUD, to narrow the area of interest for future lateritic bauxite exploration.

The (EUD and THDR) maps were then superimposed on the geologic map to geo-reference areas with dominant charnockite.

Ground investigation base on the aeromagnetic interpretations was carried out using ERT, adopting Wenner electrode array configuration with the aid of ABEM SAS1000 equipment. The coordinates of measurement station were taken using Garmin GPS. Five (5) traverses were established at 45 m inter-traverse separation (Fig. 3) and 100 m traverse length. This separation and traverse length were adopted due to the ruggedness of the terrain and the inaccessibility of most of the survey area. Traverses were laid in the NW–SE direction to image the lateritic bauxite deposit found in the study area. ERT data were processed in both 2D and 3D using Res2DInv and Res3DInv software. Both the 2D and 3D data were inverted using the least squares method. The 3D data set was generated by merging the entire orthogonal set of 2D lines established to form a single one. This was carried out by collating the measured apparent resistivity values in XYZ format that can be read by the RES3DInv software to produce a 3D model of the subsurface. Generally, interpretation was done qualitatively and quantitatively. Qualitative interpretation involves visual inspection of pseudo-section and maps. Quantitative interpretation involves the diagnosis of parameters and values obtained from the pseudo-section and maps.

4 Results and discussion

4.1 Qualitative and quantitative interpretation of aeromagnetic map

4.1.1 Total magnetic intensity (TMI) map

The TMI map (Fig. 4) shows low magnetic zones (deep blue colour-coded which range from – 938.1 to – 116.1

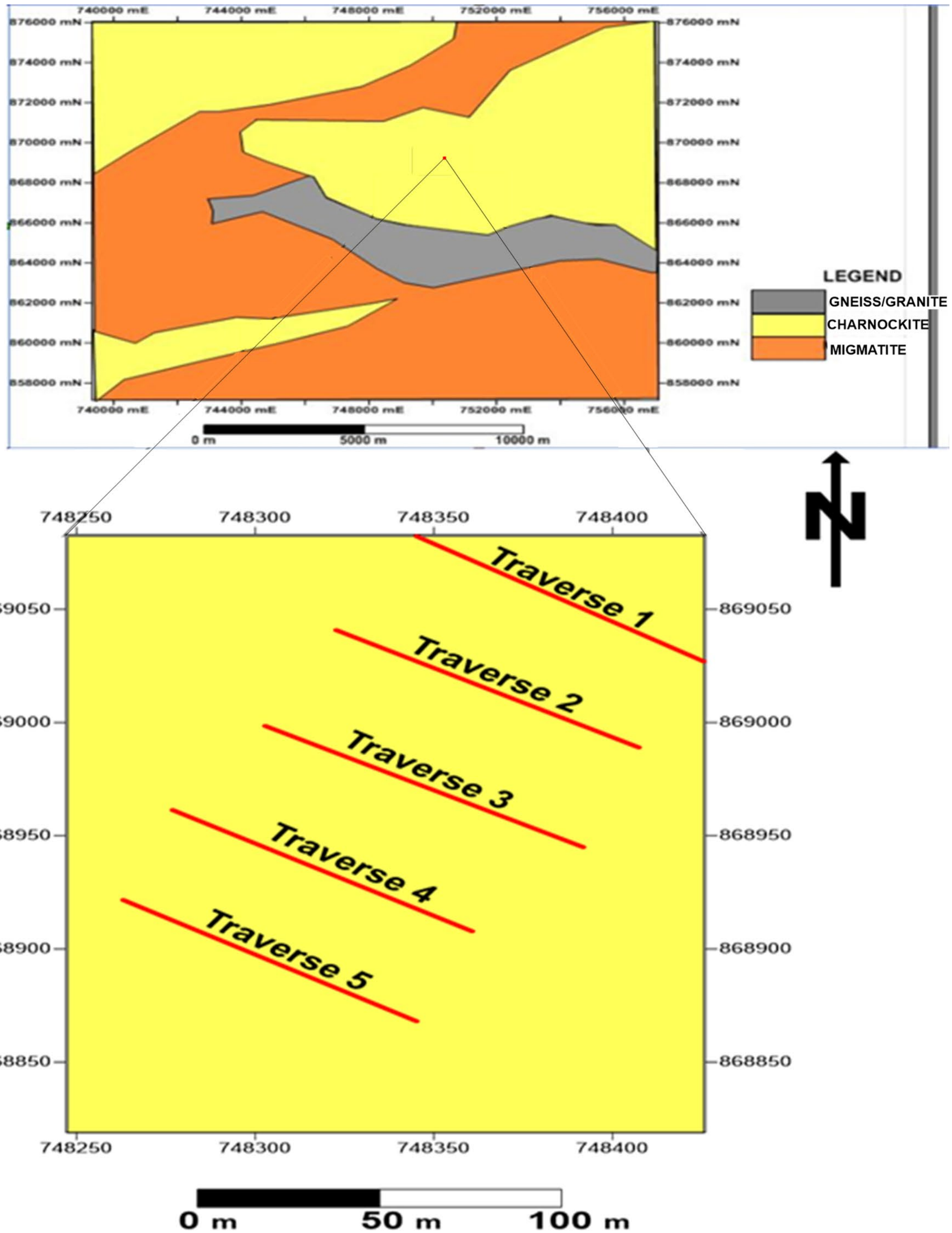

Fig. 3 Survey map of the study area

nT) appearing in the north-eastern part of the study area, light blue/green to yellow colour (which range from − 86.3 to 48.0 nT) observed, also show magnetic low to intermediate magnetic dominated areas majorly in the south-western and the north-western part of the study area, which correspond with the magnetic high/magnetic high to intermediate region (which range from 54.7 to 460.7 nT) as observed in Fig. 4, denoting areas of high concentration of lateritic bauxite.

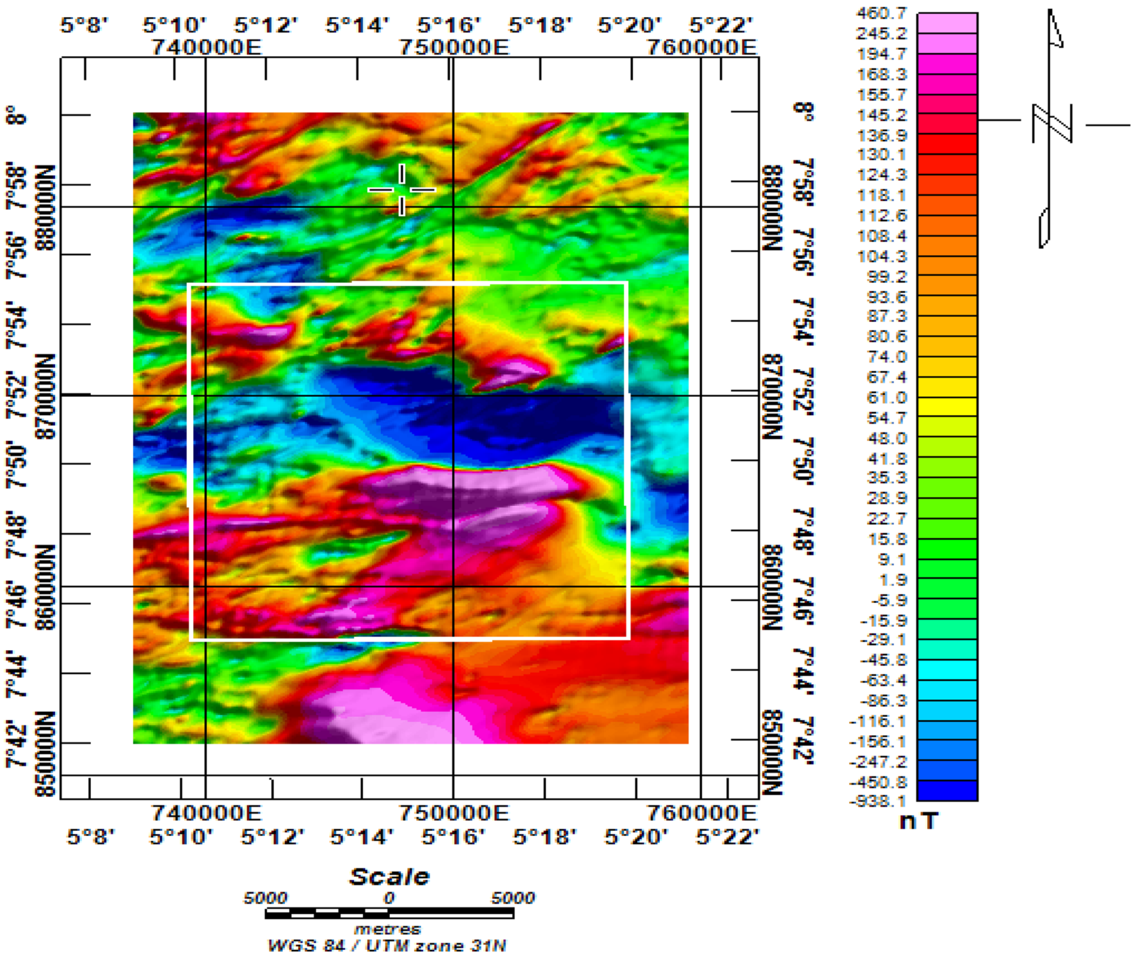

Fig. 4 TMI map of the study area

4.1.2 Reduction to the equator (RTE) map

The RTE analysis was done on the extracted magnetic anomaly data by using an assumed declination, *D*, of − 1.301 and inclination, *I*, of − 10.2950 using the international geomagnetic reference field (IGRF) calculation. The TMI comprises near-surface noise (cultural noise); this was removed using RTE. It is observed that RTE map appears smoother (Fig. 5) when compared with TMI map (with a significant difference in the low magnetic zones from − 938.1 to − 908.7 and high zones which ranges from 460.7 to 689.5). The magnetic anomalies removed from the RTE map vary in amplitude from − 908.7 to 689.5 nT, with the magnetic high occurring over granite gneiss, migmatite gneiss and magnetic low were noticed over charnockitic rock which shows the area of interest for lateritic bauxite occurrence. In this study, RTE was done on the magnetic data to sustain the low angle of inclination at the equator which converts the magnetization source to horizontal [10]. Reduction to the pole (RTP) analysis was not carried out on the magnetic data since the study location falls within a low latitude region in which there is instability in RTP transformation [10, 11]. The RTE image presented (Fig. 5) is compared to the TMI map of the study area (Fig. 4) due to the low angle of inclination of the area.

Figure 5 shows important magnetic zones were delineated from the magnetic intensity. The northern, north-western and the north-eastern parts are characterized by high amplitude magnetic anomalies similar to mafic rocks, while the southern part has low magnetic amplitude anomalies diagnostic of poorly magnetized felsic rocks.

4.1.3 Residual magnetic anomaly (RMA) map

This map shows the variation in the magnetic intensity of the different rocks across the study area (Fig. 6). Residualization was performed on the magnetic data to remove the effect of the regional field by upward continuation to a height of 2000 m and the result from the values observed

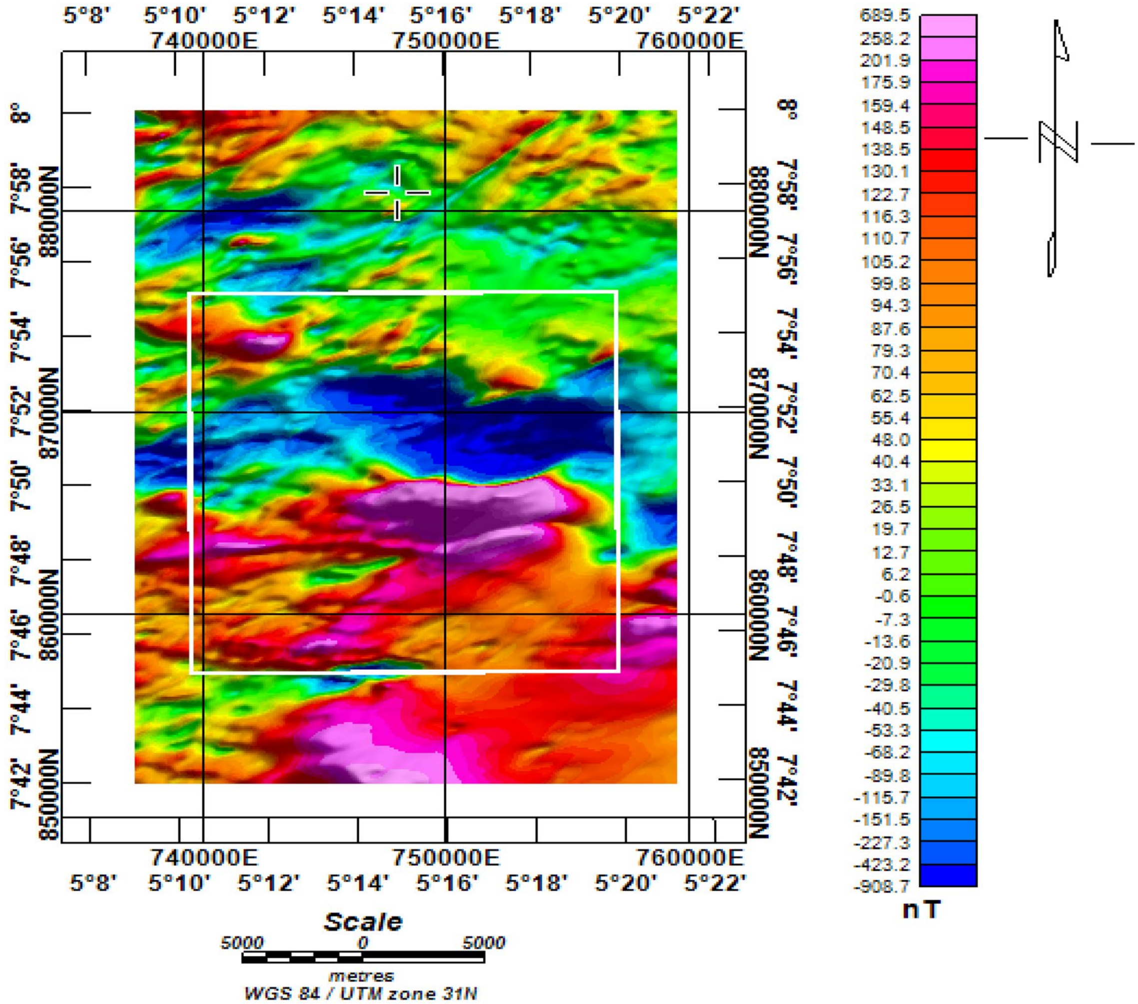

Fig. 5 Reduction to the equator (RTE) map

was removed to leave the near-surface effects which are the target for bauxitic mapping.

The resultant magnetic anomaly map obtained from residualization (Fig. 6) revealed that the main low magnetic anomaly trends are majorly in the NE–SW direction with values from – 921.4 to 97.2 nT. Magnetic highs were observed in low magnetic zones at different section within the study area. From the observed low magnetic latitude in the NE–SW region of the study area, these magnetic lows suggest rocks with comparatively low magnetic susceptibility. Magnetic highs with intensity value between 655.1 and 106.3 nT are in the northern, north-central and the southern parts (as depicted by pink colour-code) and this suggests the occurrence of rocks with relatively high magnetic susceptibility diagnostic of crystalline basement rocks (granite and migmatite gneiss). On the other hand, the north-eastern and north-western parts are controlled by the low magnetic intensity with equivalent magnetic intensity value between – 921.4 and 7.9 nT indicating the presence of relatively poor magnetic susceptibility material (weathered material, for example, laterite) overlying the basement rocks.

4.1.4 Total horizontal derivative (THDR) map

THDR filtering technique is an active instrument in discovering limits of magnetized structures [12, 13] and it also amplifies near-surface (shallow) anomalies. Figure 7 shows that THDR map above the lateritic bauxite deposit in Orin Ekiti has gradients between 0.000213 and 1.842315 nT/m. The function gives the highest point of anomaly above the contacts for magnetic anomalies [14]. The map shows peaks in the total horizontal gradient (THG) anomalies which are indicative of geologic structures which when overlaid on the geologic map of the area depicts charnockitic region/area of interest of bauxite deposit. The observed THG patterns (depicted with pink to red colour-code in Figs. 7 and 8) suggest

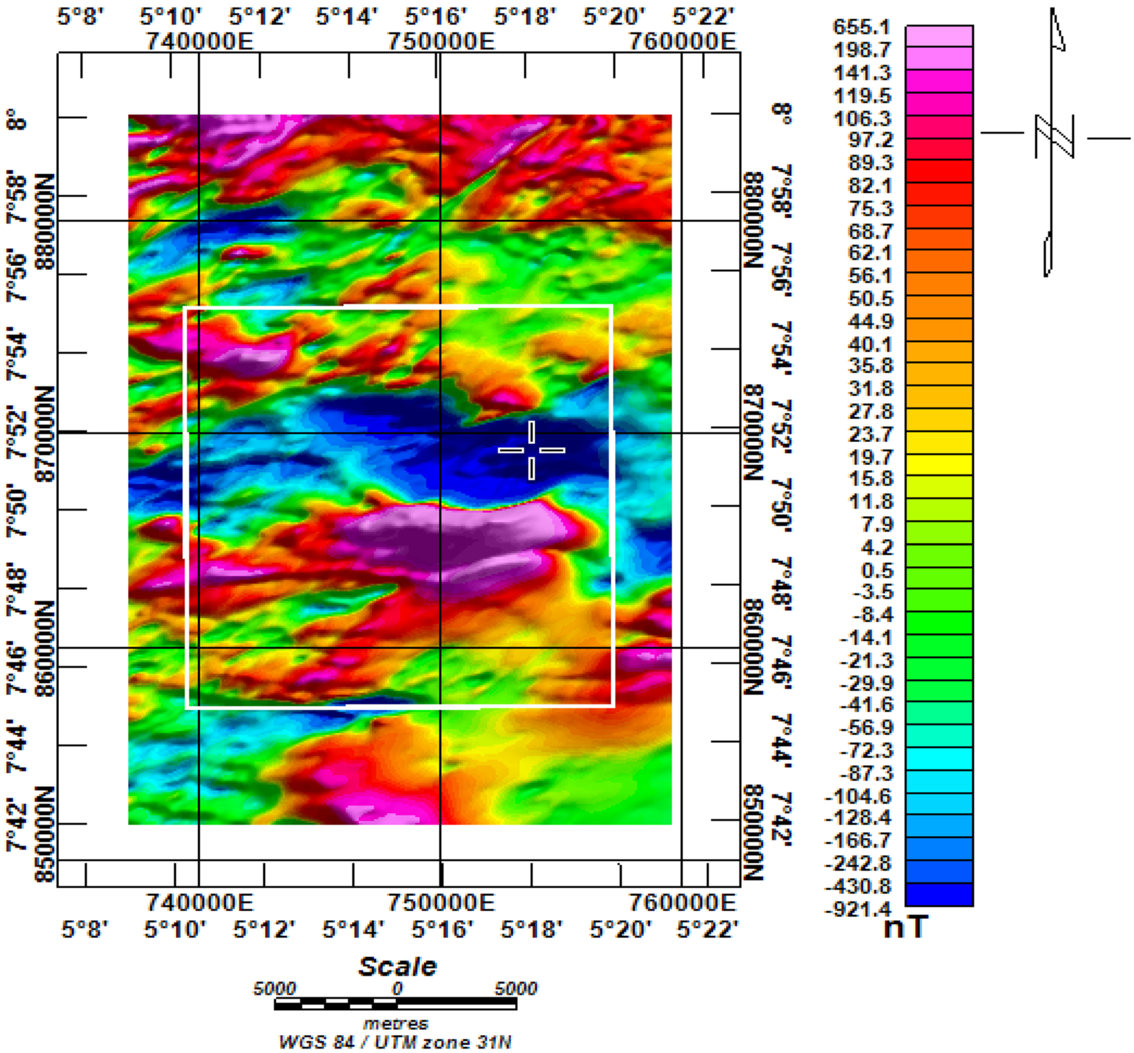

Fig. 6 Residual map

that the lateritic bauxite deposit in the area is a surficial deposit and the THG crests are the probable location of bauxitic occurrence. More so, some continuous peaks of semi-regional to regional trend (identified with white thick lines in Fig. 8) observed over the THDR map are noted to coincide with rock contacts on the geologic map. These were taken to be boundaries between rock units in the study area. These boundaries were mapped out so that rock units associated with bauxite deposits can be isolated and the area can be focused on for detailed follow-up exploration work. Other peaks (denoted with black short lines, Fig. 8) of local to semi-regional scale not vividly associated with rock or lithologic boundaries were also observed on the THDR map. These were taken to be an expression of fractures (joints/faults) and stress patterns on the immediate subsurface.

4.1.5 Euler deconvolution (EUD) map

Lineaments (Fig. 9) were generated from EUD, which was correlated with the geologic map. Structural index (SI) of 0.5 windows 5 was adopted in the calculation of depth to magnetic sources (DMS) using EUD technique. The structural index used indicates contact as a geologic model (Table 1). The EUD of the aeromagnetic data at SI of 0.5 reveals close-fitting clusters of solution characteristic of features between two rock contacts. Values between < 150 and > 300 m were projected as depth to these features (Fig. 9).

Identified rock contacts trend majorly NE–SW as observed when the SI solution was compared with the TMI map. The suggested depth to bauxitic deposits submits that lateritic bauxite deposit occurs at shallow depths.

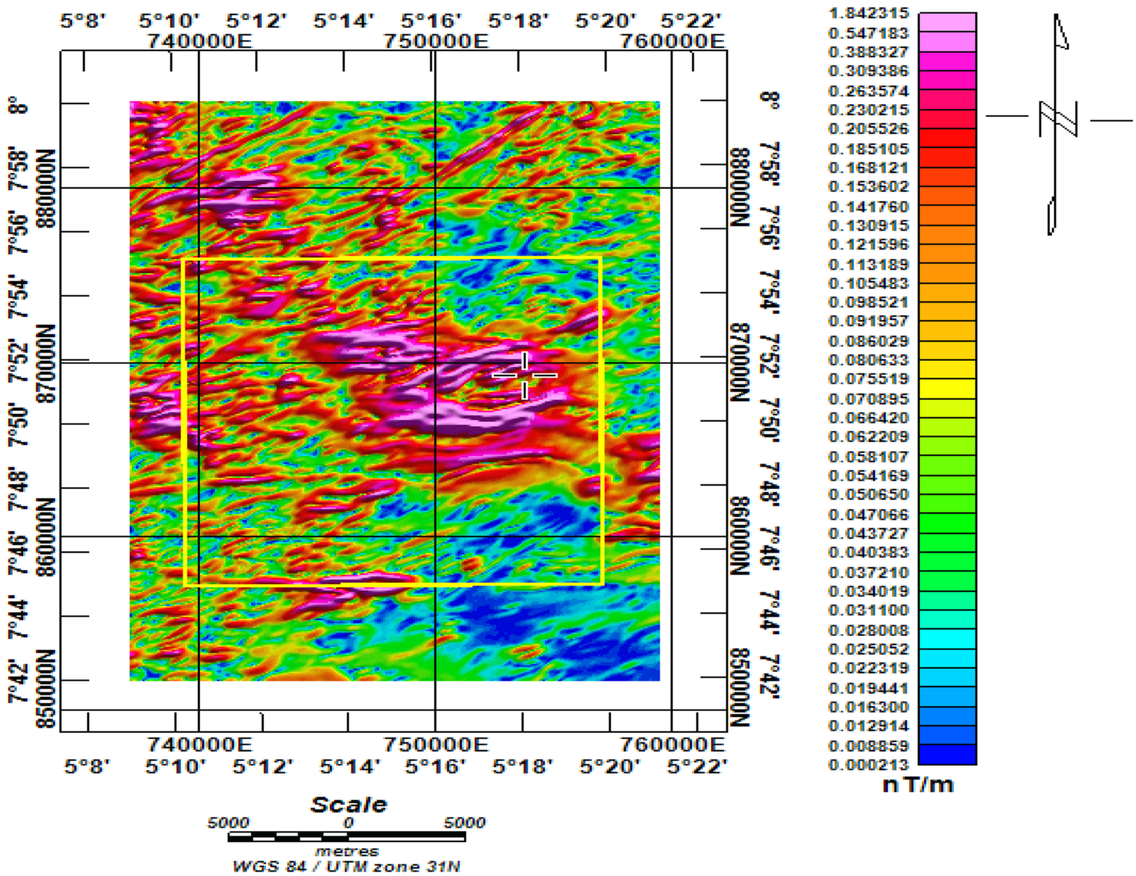

Fig. 7 Total horizontal derivative (THDR) map

4.1.6 Area of interest (AOI) map of Orin Ekiti

Figure 10 shows the lateritic bauxite potential map of NE–SW part of Orin Ekiti produced from the 3D EUD, THDR and geologic map. Zones, where the identified contacts on the geologic map match with Euler analysis on the structural index 0.5 in relation to zones with peak anomalies on the THDR, are representative of bauxitic zones. The bauxitic zones also show potential parts where ore deposits can be assessed such as the NE, the SE and the NW part of the area (Fig. 10). The depth extent estimates and structural pattern (Fig. 9) inferred with colour-code blue, green and red show cluster of blue colour-code to be more in the south-western and north-eastern part of the study area, with depth extent being less than 150 m. This reveals that significant deposit in the area lies at shallow depth which tallies with the geology of bauxite as being a supergene enrichment (surficial deposit).

The superposition of the THDR map, EULER map, with the geologic map of the area reveals that lateritic bauxite deposit is grouped more with the charnockite than with migmatite or granite gneiss rock types (Fig. 10).

4.2 2D electrical resistivity tomography (ERT)

ERI of the study area was conducted by concentrating on the charnockite-dominated region (Fig. 11) from the AOI map (Fig. 10). The 2D resistivity imaging results (Figs. 11–15) obtained from five (5) traverses established in the study area show varying resistivity values beneath the traverses with a different colour ensemble.

4.2.1 Traverse 1

This profile shows high resistivity zone which ranges from 506 to 1434 Ω m depicted with colour red at station number 17–33. The high resistivity zone indicated the presence of weathered material (laterite), hosting bauxite deposit. The blue and green colour bands which have resistivity stretching from 120–245 to 363–536 Ω m, at stations 10–25 near the surface (to the depth of 3.75 m), stations 43–60 to the depth of 10 m, stations 66–85 to the depth ranging from 1.25 to 12.5 m show that some parts of the study area with low resistivities have a surficial manifestation of migmatite gneiss and granitic rocks (unaltered parent rocks) with considerably lower resistivity than the

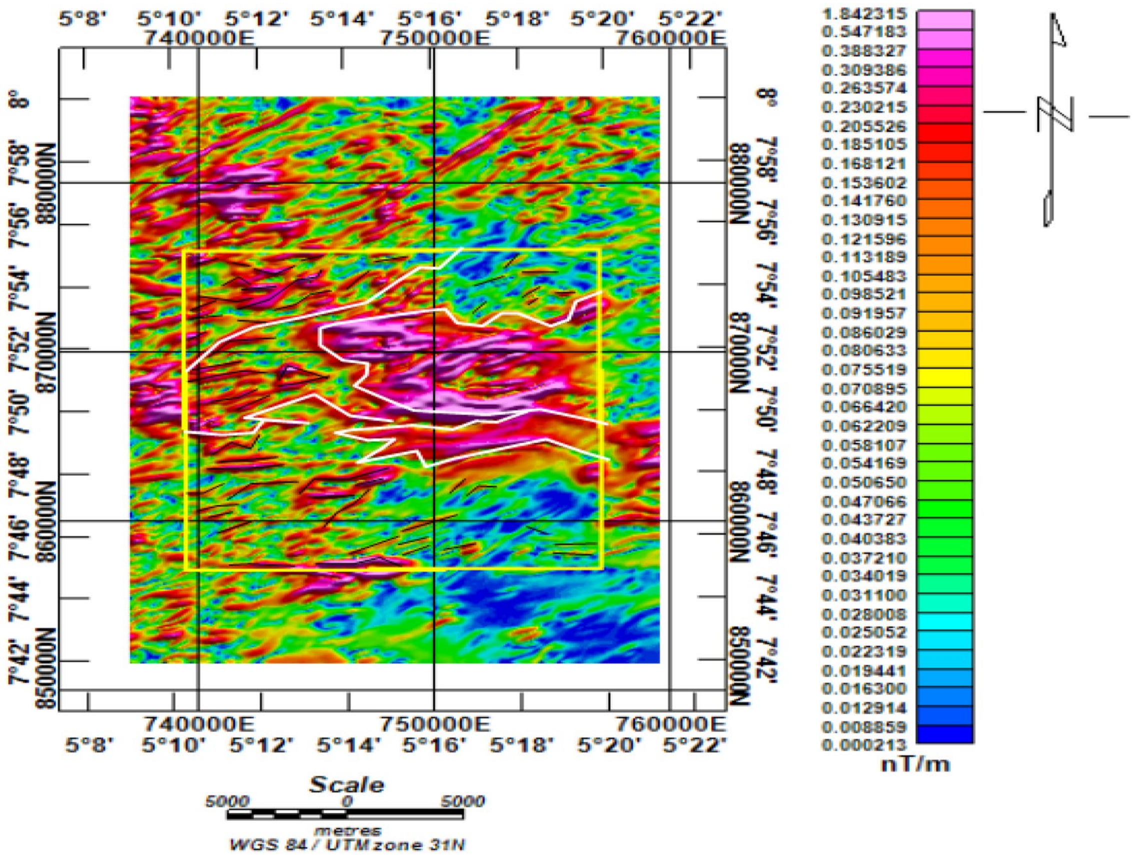

Fig. 8 Total horizontal derivative (THDR) map showing lithologic contact

weathered charnockitic rock and by extension bauxitic ore. The high resistive zone falls above the 1434 Ω m which indicates up to a depth of 3.75–12.4 m. This also displays surficial manifestation of bauxite occurrence although with considerable deeper depth (Fig. 12).

4.2.2 Traverse 2

The bauxitic zone extended almost throughout the traverse laid with a resistivity ranging from 546.5 to 1300 Ω m from station number 27 to 90 and a depth extent ranging from 2.5 to 12.4 m. The manifestation of this high resistivity zones was observed to thin-off. Zones with resistivity ranging from 225 to 451 Ω m at stations 7–90 are an indication of areas with fewer or no bauxite deposit (Fig. 12). Low resistivity region at station number 7–25, 25–33 and 67–75 with green and blue colour band, respectively, showed contact between different rock types.

4.2.3 Traverse 3

The high resistivity zones indicating lateritic bauxite with the value range from 935 to 3814 Ω m at station number 7–27, 32–55, 58–68 and 75–89 were observed in this traverse. Also, a discontinuity at station number 27–30, 55–58 and 68–75 is an indication of weathering in the bedrock along with a geologic structure that occurred between the different rock types. These fractures resulted in narrow weathered zones that extend deep into the bedrock. The contracted weathered zones are largely composed of saprolite and are known to commonly contain high bauxite grades [16]. The bauxitic zones delineated (Fig. 13) are the ferricate zone formed by the placement and crystallization of surficial limonite in surface acidic condition. The ferricate cap is very hard and shows high porosity, parched of bound water, and is known to be highly electrically resistive [17]. Imaging on this traverse, however, indicates the exposure and the downward extension of the hard and compact bauxite deposit. The depth of occurrence ranges from the surface to as far as 12.4 m deep, which thin out at station 16–27.

4.2.4 Traverse 4

The 2D images were interpreted vis-a-vis the textural features and the earlier discussed colour regimes (Fig. 14).

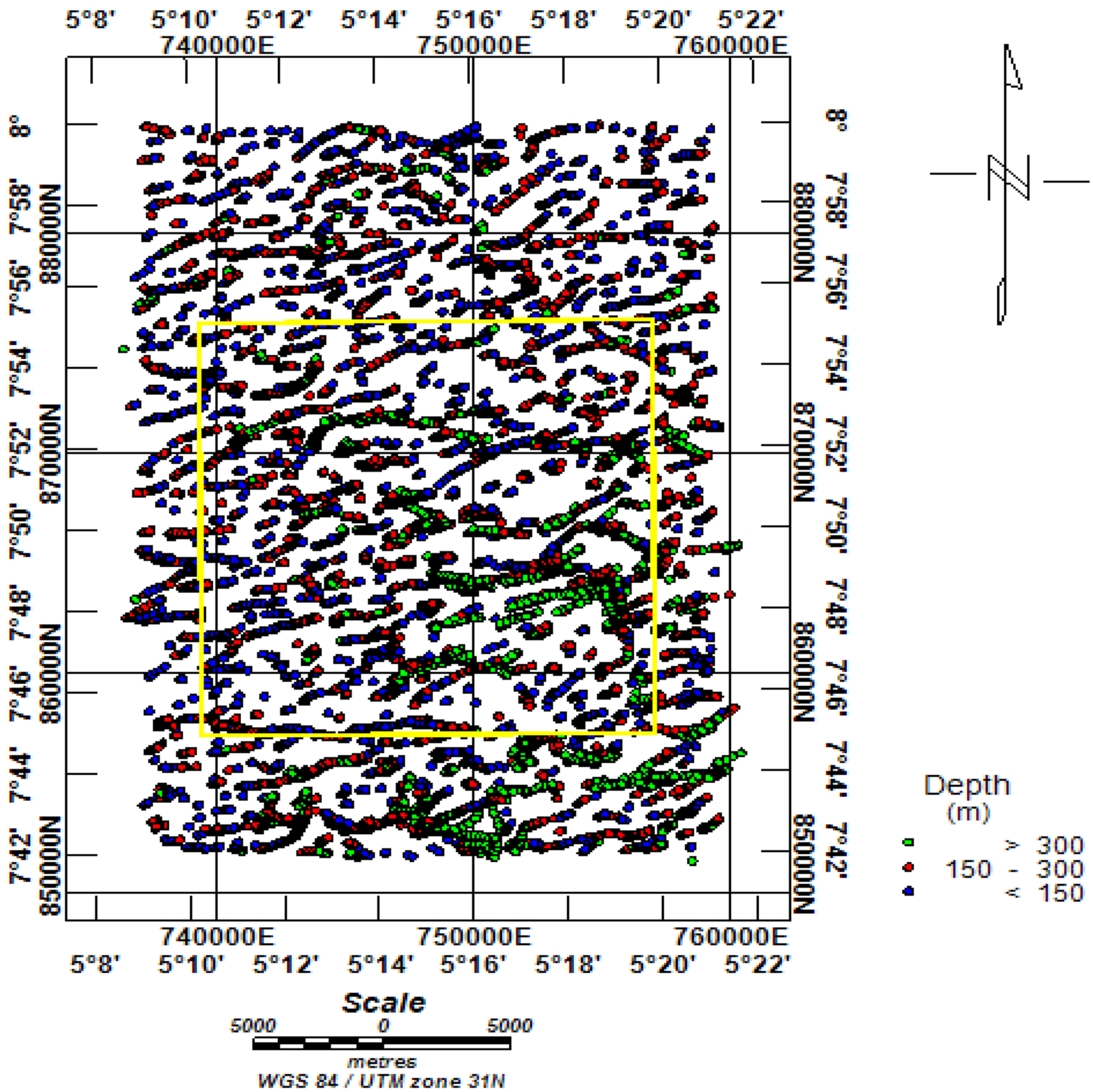

Fig. 9 Euler deconvolution (EUD) map (SI = 0.5, WIN 5)

Areas (stations 13–18 and 25–77) under green colour bands within the upper and middle layers of the pseudo-section constitute the topsoil/lateritic layer, while similar zones present to the depth of about 9.94 m represent the lateritic bauxitic zones which extend from stations 35 to 67. The high resistive zones in this profile (342–2566), furthermore, show the rate of the degree of weathering along the established traverse and by extension the increase in the presence of lateritic bauxite.

Table 1 Structural indices for geologic models *Source* : [15]

Structural index	Geologic model
0 (0.5)	Contact
1	Sill
1	Dyke
2	Horizontal cylinder
2	Pipe
3	Sphere

4.2.5 Traverse 5

The reddish colour band (Fig. 15) which thin out eastward from stations 55 to 85 in the vicinities of the purple colour band is suggestive of the resistivity characteristics of the granular bauxite ore [5]. Meanwhile, areas under the yellowish/greenish colour bands especially those beneath the depths of about 10 m and directly

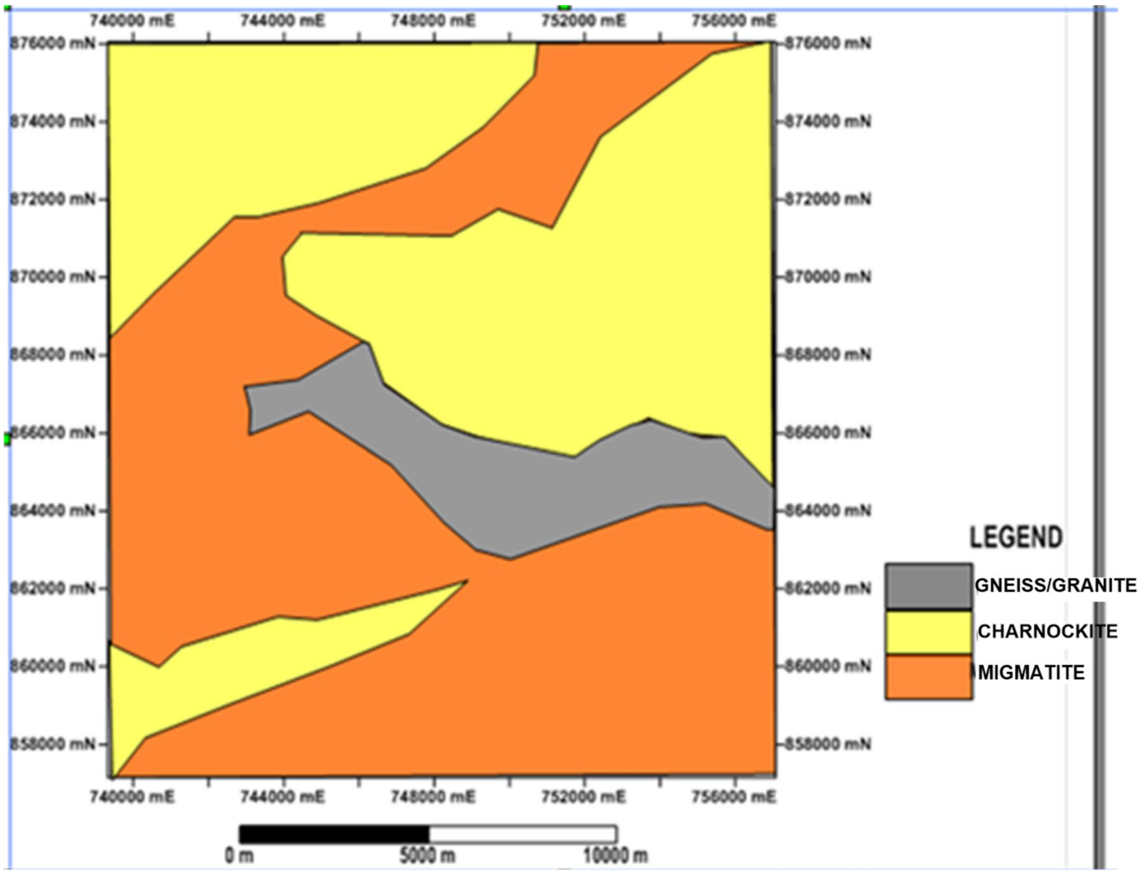

Fig. 10 Geologic map from Euler deconvolution analysis and THDR

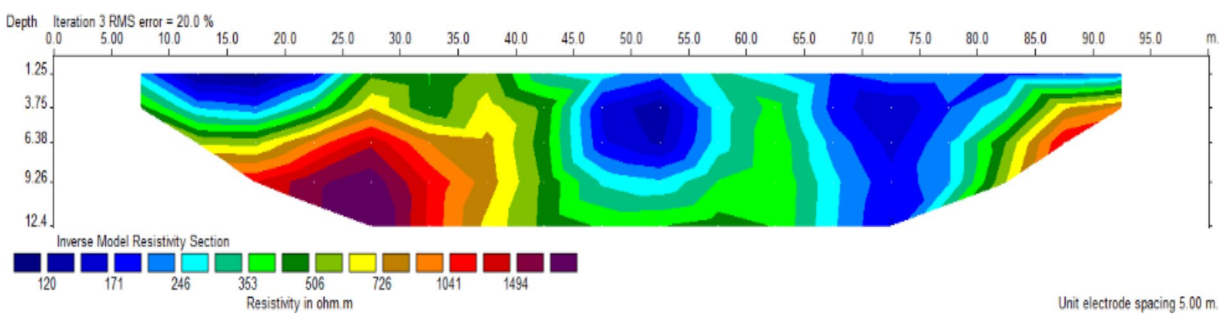

Fig. 11 2D pseudo-section along traverse 1

beneath the earlier identified granular bauxites are suspected to emanate from the friable/stippled bauxite ore. The resistivity (with the range of 968–2566 Ω m), which depicts the bauxite zones at stations 55–85 at a depth ranging from 1.25 to 11.5 m, showed very high resistivity at the eastern part of the survey area.

4.2.6 3D electrical resistivity imaging (ERI)

Figure 16 shows the 3D model resistivity values in horizontal depth slices in *y–z* direction. The 2D images of the five (5) traverses (Figs. 11–15) agree with the inversion model of the 3D inversion image. For example, stations 15–25 and

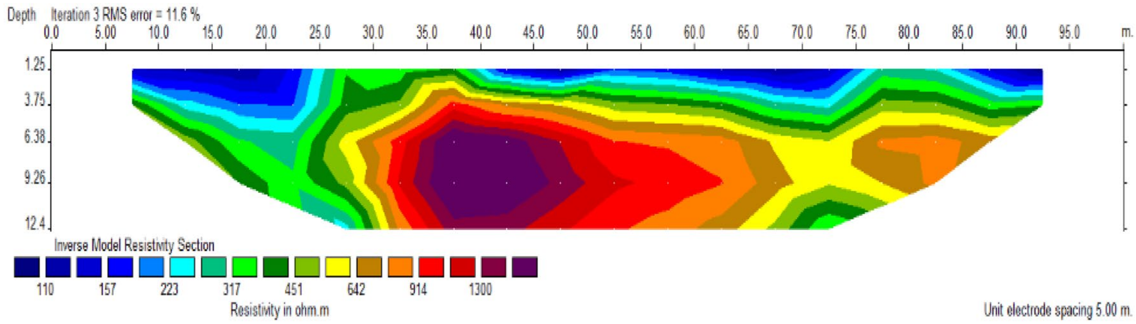

Fig. 12 2D pseudo-section along traverse 2

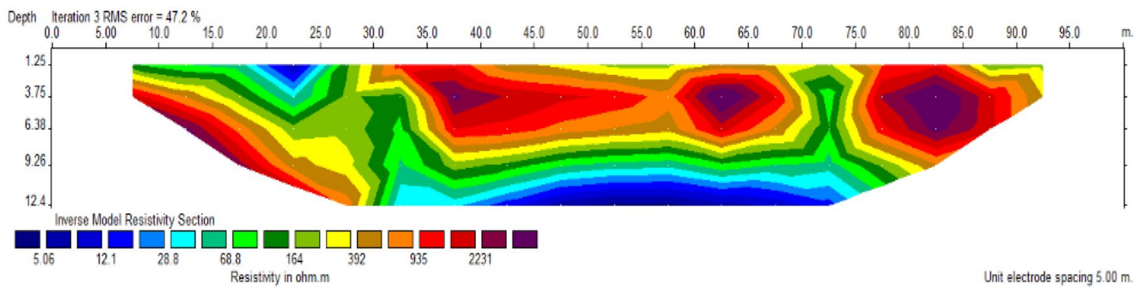

Fig. 13 2D pseudo-section along traverse 3

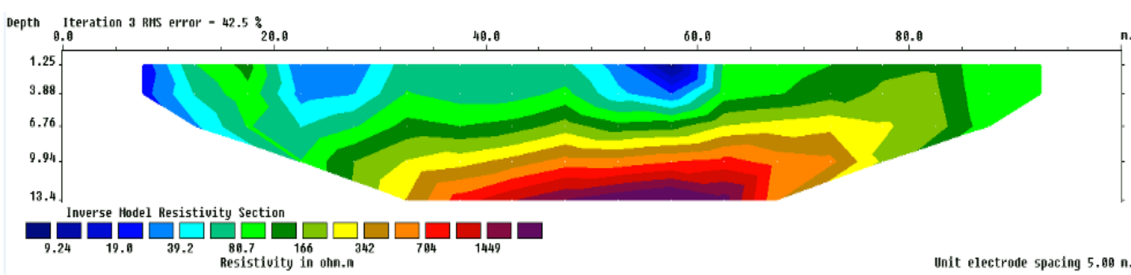

Fig. 14 2D pseudo-section along traverse 4

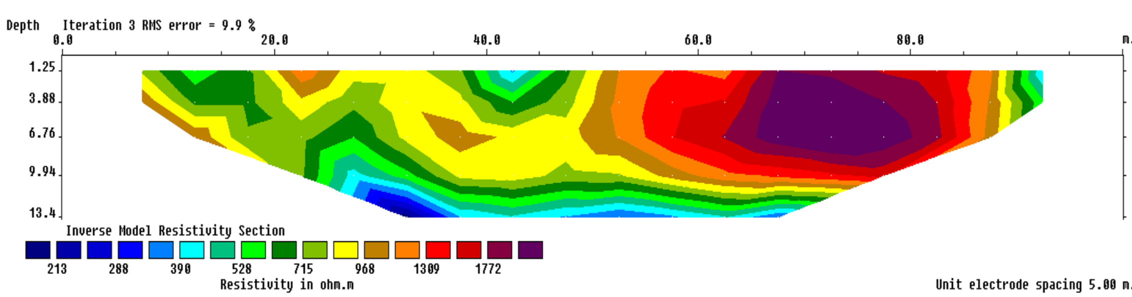

Fig. 15 2D pseudo-section along traverse 5

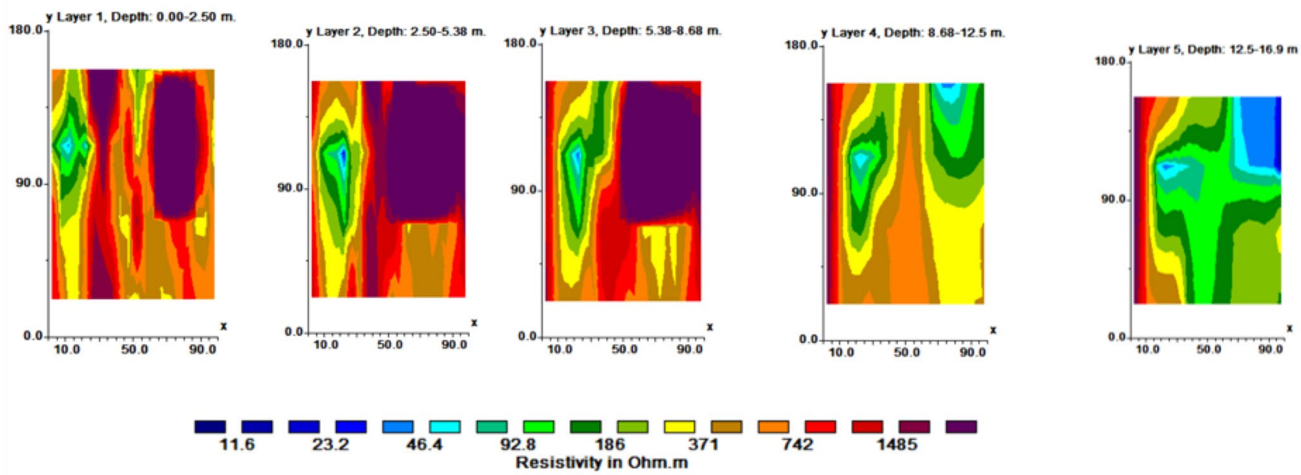

Fig. 16 3D imaging showing resistivity distribution of the electrical resistivity survey

85–95 in traverse 1 correspond well with the same points in layer 1 on the 3D image with a high resistivity. There is an increase in the degree of consistency of the resistivity distribution in both the 2D and 3D images, that is, both 2D and 3D images are complementary to each other. False information that may be associated with 2D inversion has been taken care of in the image displayed in 3D. The depth extent in both 2D and the 3D image shows that bauxitic deposits have surficial manifestation.

5 Conclusions

From the HRAD, raw TMI map was generated in which different filtering techniques which were carried out to enhance better understanding of the study area, with the generation of different maps therein. Low magnetic intensities were observed over charnockitic rock. Low magnetic anomaly trending NE–SW exists. The EUD and THDR maps generated from the HRAD were then superimposed on the geologic map to geo-reference areas that have dominant charnockite which is a host material for bauxite occurrence.

The AOI map generated for lateritic bauxite shows the interest region to be NE–SW parts. The depth extent estimates and structural pattern interpreted from magnetic anomalies reveal that considerable deposit within the area lies at shallow depth which tallies with the geology of bauxite as a surficial deposit.

The overlay of the THDR map, EULER map, with the geologic map of the area also suggests that lateritic bauxite deposit is related more with the charnockite than with migmatite or granite gneiss rock types.

The 2D and 3D resistivity imaging results obtained from five traverses show that bauxite deposit is surficial and the bedrock interface is not even. The images display the unbroken resistivity regimes beneath the traverses with a divergent colour ensemble. The 2D and 3D images for traverse 1–5 show high resistivity zone which ranges from 154–3814 to 371–2600 Ω m, respectively, depicted with the colour red to purple, thereby emphasized the area of interest for lateritic bauxite manifestation. The high resistivity zone indicated the presence of weathered material (laterite), hosting bauxite deposit. The blue and green colour bands which have resistivity stretching from 53.8–290 to 124–279 Ω metre, respectively, show that migmatite gneiss and granitic rocks (unaltered parent rocks) are of considerably lower resistivity than the weathered charnockitic rock and by extension bauxitic ore. The present study is essentially a near-surface investigation in which a maximum investigation depth of 16.9 m is reached as shown in the 3D inversion displayed. The different techniques used in this study have, furthermore, shown that the area of interest for bauxitic deposit in Orin Ekiti trends in the NE–SW direction with a dominant concentration in the north-eastern part. By the same token, this research has been able to open the field of Orin for more research work on lateritic bauxite and also substantiate the fact that bauxite deposits occur as supergene enrichment.

Funding This research work is funded by the Tertiary Education Trust Fund (TETFUND).

Compliance with ethical standards

Conflicts of interest There is no conflict of interest among the authors.

References

1. Odeyemi IB (2001) Minerals and man: an inseparable duo. In: Saliu NB (ed) Nigerian universities inaugural lecture series 2001. National Universities Commission, Abuja, pp 567–587
2. Ajaka EO, Oyethelemi EO (2010) Suggesting area for investigation of mineral occurrence database. ARPN J Eng Appl Sci 5(11):27–39
3. Plunkert PA (2000) Bauxite and Alumina. US Geological Survey Minerals Yearbook
4. Talabi AO, Ademilua OL, Ajayi OZ, Ogunniyi SO (2013) Preliminary geophysical evaluation of orin bauxite deposit southwestern Nigeria. J Emerg Trends Eng Appl Sci 4:432–437
5. Eluwole AB, Ademilua OL, Oyinloye A, Adebayo OF, Obasi RA, Talabi AO, Olaolorun OA (2019) Geoelectric assessments of the bauxite ore deposit at orin-ekiti, southwestern Nigeria. Int J Appl Environ Sci 14(2):197–210
6. Talabi AO, Oyinloye AO, Olaolorun OA, Obasi RA, Eluwole AB, Adebayo OF, Ademilua OL (2018) Petrography and geochemistry of orin-ekiti basement rocks, southwestern Nigeria: implications on bauxitization. Am J Appl Sci 15(4):230–239
7. Reid AB, Allsop JM, Granser H, Millet AJ, Somerton IW (1990) Magnetic interpretation in three dimensions using euler deconvolution. Geophysics 55(1):80–91
8. Thompson DT (1982) EULDPH – a new technique for making computer-assisted depth estimates from magnetic data. Geophysics 47:31–37
9. Cordell L, Grauch VJS (1985) Mapping basement magnetization zones from aeromagnetic data in the San Juan basin, New Mexico. In: Hinze WJ (ed) The utility of regional gravity and magnetic anomaly maps. SEG, Tulsa, pp 181–197
10. Ndousa-Mbarga T, Fenmoue ANS, Manguelle-Dicoum E, Fairhead JD (2012) Aeromagnetic data interpretation to locate buried faults in south-east cameroon. Geophysica 48(1–2):49–63
11. Rajagopalan S (2003) Analytical Signal vs reduction to pole: solutions for low magnetic Latitudes. Explor Geophys 34:257–262
12. Keating P, Pilkington M (2004) Euler deconvolution of the analytic signal and its application to magnetic interpretation. Geophys Prospect 52:165–182
13. Cooper GRJ (2009) Balancing images of potential field data. Geophysics 74:17–20
14. Oyeniyi TO, Salami AA, Ojo SB (2016) Magnetic surveying as an aid to geological mapping: a case study from obafemi awolowo university campus in Ile-Ife, southwest Nigeria. Ife J Sci 18(2):331–343
15. Geosoft (2005) Montaj GridKnit, Grid extension for OASIS Montaj 6.1. Tutorial and User Guide, Geosoft Incorporated, 27
16. Golightly FA, Stott FH, Wood GC (1979) The relationship between oxide grain morphology and growth mechanisms for Fe-Cr-Al and Fe-Cr-Al-Y alloys. J Electrochem Soc 126(6):1035–1042
17. Peric M (1981) Exploration of burundi nickeliferous laterites by electrical methods. Geophys Prospect 29(2):274–287